

A low cost approach for the fabrication of microwave phase shifter on laminates

Poonam Goel · K. J. Vinoy

Received: 10 June 2011 / Accepted: 10 August 2011 / Published online: 30 August 2011
© Springer-Verlag 2011

Abstract This paper presents a simple and low cost fabrication approach using extended printed circuit board processing techniques for an electrostatically actuated phase shifter on a common microwave laminate. This approach uses 15 μm thin copper foils for realizing the bridge structures as well as for a spacer. A polymeric thin film deposited by spin coating and patterned using lithographic process is used as a dielectric layer to improve the reliability of the device. The prototype of the phase shifter for X-band operation is fabricated and tested for electrical and electromechanical performance parameters. The realized devices have a figure of merit of 70°/dB for a maximum applied bias potential of 85 V. Since these phase shifters can be conveniently fabricated directly on microwave substrates used for feed distribution networks of phased arrays, the overall addition in cost, dimensions and processing for including these phase shifters in these arrays is minimal.

1 Introduction

Recent developments in the area of microfabrication technologies, has enabled the fabrication of many radio frequency/microwave components with better performance and lower cost than possible with semiconductor based fabrication technology. Many of these microfabricated RF components such as switches and phase shifters, popularly known as RF MEMS, are aimed at reducing the insertion

loss and improving other performance parameters such as linearity. For these devices size miniaturization is not necessarily important, as in practical subsystems, these components are integrated with RF front-ends on a laminate.

RF MEMS phase shifters can be implemented using switched line approach or distributed MEMS transmission line (DMTL) approach. In DMTL phase shifters small phase shift can be achieved with high accuracy. Demonstrated DMTL phase shifters on fused silica (McFeeters and Okoniewski 2006), high resistivity silicon (Palei et al. 2005; Lakshminarayanan and Weller 2002), low resistivity silicon (Wang et al. 2008; Guo et al. 2006), or ceramic substrates such as quartz (Hayden and Rebeiz 2003, 2000, 2002; Lakshminarayanan and Weller 2007, 2006; Barker and Rebeiz 2000, 1998; Fangmin et al. 2001), Pyrex glass (Liu et al. 2000; Borgioli et al. 2000; Topalli et al. 2006), use highly sophisticated and expensive silicon microfabrication process technologies. RF devices have also been demonstrated with several non-conventional processes on microwave laminates with emphasis on the performance improvement in insertion loss at the cost of fabrication complexity (Ramadoss et al. 2005).

This paper presents a low cost approach for the fabrication of a passive phase shifter that can be fabricated in situ on a microwave laminate. The principle of operation of this mesoscale electrostatically actuated phase shifter on microwave laminate (MEPL) is similar to that of a micromachined DMTL phase shifter. In spite of advantages of low losses, wide bandwidth, low DC power consumption and high linearity over semiconductor/MMIC technology, microfabricated phase shifters are not much used in field because of issues related to fabrication reliability, packaging and integration. On the other hand, the proposed MEPL overcomes these issues, while retaining all the advantages of conventional MEMS phase shifters.

P. Goel (✉) · K. J. Vinoy
Department of Electrical Communication Engineering,
Indian Institute of Science, Bangalore 560012, India
e-mail: poonam.goel13@gmail.com

K. J. Vinoy
e-mail: kjvinoy@ece.iisc.ernet.in

Furthermore, these are integrable to form a monolithic phased array. Various aspects of the design, fabrication, and characterization of the phase shifter are discussed in the following sections.

The RF and electromechanical design aspects of the phase shifter are discussed in the next section. Some process modifications are necessary to fabricate this phase shifter on conventional microwave laminates. These are presented in Sect. 3. The measured results from the fabricated prototypes are presented along with a discussion in Sect. 4. Key features of the proposed approach are summarized in Sect. 5. Since these phase shifters are fabricated directly on microwave laminates used for feed distribution networks of phased arrays, the overall addition in cost, dimensions, and processing for including these phase shifters is very small.

2 Design of the phase shifter

The operation of this mesoscale electrostatically actuated phase shifter on microwave laminate (MEPL) is similar to that of a micromachined distributed MEMS transmission line (DMTL) phase shifter. These phase shifters are implemented by periodic loading of a coplanar waveguide (CPW) transmission line with bridge structures as shown in Fig. 1. When actuated electrostatically, the capacitance of these shunt capacitors vary, changing the phase velocity, and consequently the phase (McFeetors and Okoniewski 2006).

2.1 RF design and modelling

Assuming the transmission line to be loss-less, one may relate capacitance C_t , and inductance L_t per unit length of

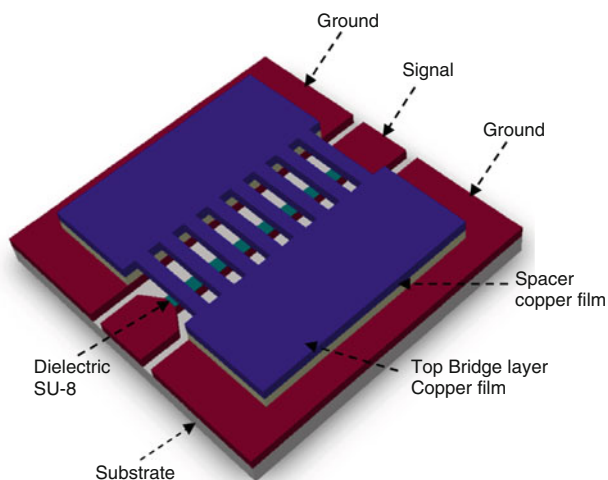


Fig. 1 Schematic of the mesoscale electrostatically actuated phase shifter on laminate

the CPW to the characteristic impedance and effective permittivity (Barker and Rebeiz 1998)

$$C_t = \frac{\sqrt{\epsilon_{\text{reff}}}}{cZ_0} \quad (1)$$

$$L_t = C_t Z_0^2 \quad (2)$$

where Z_0 is unloaded line impedance, ϵ_{reff} is effective dielectric constant of the CPW. When these bridges (shown in Fig. 1) are close enough, their capacitance can be distributed over the length of the unit cell. Therefore, the length of the unit cell or the spacing between bridges (s) should be much smaller than a wavelength. The maximum spacing between bridges is decided by the Bragg's frequency ω_b which is the frequency at which the characteristic impedance of the loaded line becomes purely imaginary. Hence ω_b is generally kept 2–3 times of the maximum operating frequency. The Bragg frequency is given by (Barker and Rebeiz 1998; Palei et al. 2005):

$$\omega_b = \frac{2}{\sqrt{sL_t(sC_t + C_{b0})}} \quad (3)$$

where C_{b0} is the parallel plate capacitance between the bridge and the signal trace below. All these bridges are simultaneously deflected by the application of a bias, which is superimposed with the RF between the signal and ground traces of the CPW. This causes the bridge capacitance to vary which in turn affects the signal velocity. Phase shift per unit length is related to the resulting change in the phase constant (Rebeiz 2003):

$$\Delta\Phi = \beta_1 - \beta_2 = \omega \left(\frac{1}{v_1} - \frac{1}{v_2} \right) \quad (4)$$

where v_1 is the signal velocity without bias voltage, v_2 is the signal velocity in the deflected position of the beam and are given by:

$$v_1 = \frac{1}{\sqrt{L_t(C_t + C_{b0}/s)}} \quad (5)$$

$$v_2 = \frac{1}{\sqrt{L_t(C_t + C_d/s)}} \quad (6)$$

where C_d is the bridge capacitance in the deflected position. Therefore,

$$\begin{aligned} \Delta\Phi &= \omega \sqrt{L_t C_t} \left(\sqrt{1 + \frac{C_b}{sC_t}} - \sqrt{1 + \frac{C_d}{sC_t}} \right) \\ &= \frac{\omega Z_0 \sqrt{\epsilon_{\text{reff}}}}{c} \left(\frac{1}{Z_{lu}} - \frac{1}{Z_{ld}} \right) \text{ rad/m} \end{aligned} \quad (7)$$

where Z_{lu} and Z_{ld} are the impedance of the CPW with the original and deflected positions of the bridges. The

maximum stable deflection of the bridge is determined by the stable region of operation of electrostatic beam. Therefore, electromechanical modelling of the beam structure is discussed next.

2.2 Electromechanical design and modelling

Electrostatic actuation is based on the Coulomb’s law by which the electrostatic force (F_e) between oppositely charged plates separated by a gap g and a potential of V , is given by

$$F_e = \frac{1}{2} V^2 \frac{dC(g)}{dg} = -\frac{1}{2} \frac{\epsilon_0 w W V^2}{g^2} \tag{8}$$

where the parallel plate capacitance C depends on the position of the movable bridge electrode whose width is w . The width of the bottom electrode is W . The beam is stable as long as the electrostatic force is balanced by the beam restoring force.

$$\frac{1}{2} \frac{\epsilon_0 w W V^2}{g^2} = k(g_0 - g) \tag{9}$$

Beam restoring force is the mechanical force due to beam stiffness k . In Eq. 9, g_0 is the original height of the beam electrode above the bottom conductor. Since the Coulomb force increases quadratically as g is reduced, electrostatic force dominates the elastic restoring force once the bias voltage exceeds a certain level, and the beam becomes unstable. This phenomenon is known as pull-in which occurs at around $g = 1/3g_0$. For reliable operation of this phase shifter the deflection should be below this value. The corresponding bias voltage is given by

$$V_P = \sqrt{\frac{8k g_0^3}{27\epsilon_0 A}} \tag{10}$$

Hence electromechanical modeling of the beam structure is done to find out the pull-in voltage. For the MEPL of cross sectional structure shown in Fig. 2, this sets the maximum voltage up to which the phase shifter can be operated is:

$$V_P = \sqrt{\frac{8k \left(g_0 + \frac{t_d}{\epsilon_r}\right)^3}{27\epsilon_0 A}} \tag{11}$$

As this has a dielectric film of thickness t_d and permittivity ϵ_r above the conductor. In this design, fixed–fixed beam is deflected with a uniformly distributed force directly above the center conductor of the CPW (Rebeiz 2003). Spring constant can be obtained from:

$$k = 32Ew \left(\frac{t}{L}\right)^3 \frac{1}{8\left(\frac{x}{L}\right)^3 - 20\left(\frac{x}{L}\right)^2 + 14\left(\frac{x}{L}\right) - 1} \tag{12}$$

where E is Young’s modulus of elasticity, t is the beam thickness, L is the beam length, and $x = (L + W)/2$.

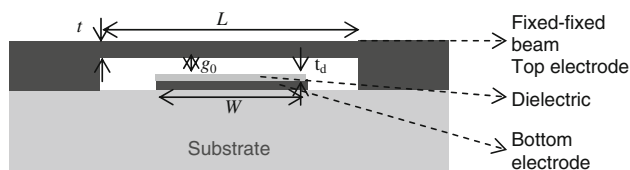


Fig. 2 Cross-sectional view of fixed–fixed beam. The electrostatic force is uniformly distributed along the width of the bottom electrode, at the centre of the beam

2.3 Design overview and simulations

The proposed approach uses a multilayer fabrication technique to realize the phase shifter shown in Fig. 1. In this, CPW is patterned on the microwave laminate. In order to make the characteristic impedance of the loaded CPW about 50Ω , the dimensions of the CPW are determined. The signal width is kept at $2,400 \mu\text{m}$ at the ends of the transmission line to facilitate soldering of SMA connectors. In the middle region this width is kept at $500 \mu\text{m}$. The slot between the signal and ground traces there is $1,250 \mu\text{m}$. The ground conductor is wide ($4,000 \mu\text{m}$) enough to contain all fields.

In order to minimize the fabrication cost, the bridge structures are realized using a copper foil and are attached to this CPW. The spacer between beams and CPW is also realized with the same material. Therefore, the height of beam is $15 \mu\text{m}$ above the bottom conductor. The lateral dimensions of conductors are decided by the limitations of printed circuit board processing by lithography. Based on this constraint, the beam width is chosen to be $200 \mu\text{m}$. The design parameters of the realized device are listed in Table 1. Several fabrication steps were developed to meet these challenges during the fabrication of MEPL, as discussed in the next section.

Coventorware which is a finite element method based electromechanical simulation software, is used for an

Table 1 Values of design parameters of the fabricated prototypes

Design parameters	Values
Beam thickness (μm)	15
Beam length (μm)	4,000
Beam width (μm)	200
Bottom electrode (CPW) width (μm)	500
Beam spacing (μm)	350
CPW ground width (μm)	7,400
Slot between ground and signal of CPW (μm)	200
Spacer thickness (μm)	15
Dielectric thickness (μm)	4
Dielectric constant of SU8	4
Young’s modulus of copper (GPa)	128

accurate modelling incorporating the effects which were not included in the analytical approach discussed in the previous section. The pull-in voltage for this configuration is found to be 106 V. For a complete understanding of the behaviour of this device full wave EM simulations are performed using CST microwave studio. The Bragg's frequency of the modelled device is 59 GHz. The phase shift per unit cell is 3.2° at 10 GHz. The insertion loss of this device is better than 1 dB and the return loss is better than 15 dB.

3 Fabrication of the phase shifter

The mesoscale electrostatically actuated phase shifter on the microwave laminate (MEPL) is fabricated using the laminate Arlon AD250 of height 60 mils with dielectric constant 2.5 is used as the substrate material. The microwave laminate is first cleaned by soft rubbing with a scrub and dipping for 1 min in 10% sulphuric acid (H_2SO_4). After this, the sample is thoroughly washed with the deionized (DI) water to remove the acid contents and kept in the oven for 5 min at 80°C to dehydrate. The laminate is patterned for CPW dimensions (Table 1) by a print and etch technique using a dry photo-resist film. Wet chemical etching of CPW is done with ferric chloride (FeCl_3).

In order to minimize the fabrication cost, the bridge structures are realized using a copper foil and are attached to this CPW. Since the spacer between beams and CPW is also realized with the same material, the height of beam above the bottom conductor is $15\ \mu\text{m}$. Some process modifications were required to realize devices with consistent performance. For example, in order to prevent electrostatic breakdown, a spin coated dielectric film is included in this design. We have used SU-8 which is reported to have good dielectric strength. The surface roughness of copper on the laminate caused inconsistencies in the measured dielectric strength which was improved by *polishing of copper*. *Patterning of beam structures* on the

thin copper foil was another challenge. Photochemical milling was found to give good results in this regard. These are discussed in the following paragraphs.

3.1 Polishing of copper on laminate

The surface roughness can be evaluated using measurements using profilometers. The laminate used for the fabrication is found to have a roughness of $\pm 3\ \mu\text{m}$ (Fig. 3). Approaches to reduce the surface roughness of the microwave laminates include polishing and planarization and compressive molding planarization (Ghodsian et al. 2005) which needs polyamide coating. We polished the laminate directly without the polyamide film. The laminate is polished very carefully after patterning the CPW because as the width of the signal conductor trace is very narrow. Polishing is done utilizing Grinder-polishing machine. First, microwave laminate surface is polished with fine carbon particle paper and then using a diamond paste on a nylon cloth. As shown in Fig. 4, the peak to peak surface roughness is reduced to less than $0.7\ \mu\text{m}$ with this approach. Electrical tests to measure the dielectric strength of the SU-8 spin coated on the polished microwave laminate samples showed dielectric strength of greater than 300 V for $4\ \mu\text{m}$ of SU-8 which meets the present requirement.

3.2 Depositing dielectric layer on the laminate

Most of the previous attempts to realize mesoscale devices on laminates used vacuum deposited thin films (Ramadoss et al. 2006). In the present approach, an epoxy based polymer film is used as the dielectric layer. SU-8, an epoxy based negative photo-resist which is used to make high aspect ratio structures in microsystems, is resistant to solvents, and has excellent thermal and structural stability. Polished microwave laminate metallization layers is spun with SU8 (Microchem) at 500 rpm for 35 s with acceleration of 200 rpm/s, pre-baked at 65°C temperature for

Fig. 3 Surface profile measurements with Wyko optical profilometer on the laminate before polishing. **a** 3D-image and **b** linear scan measurement

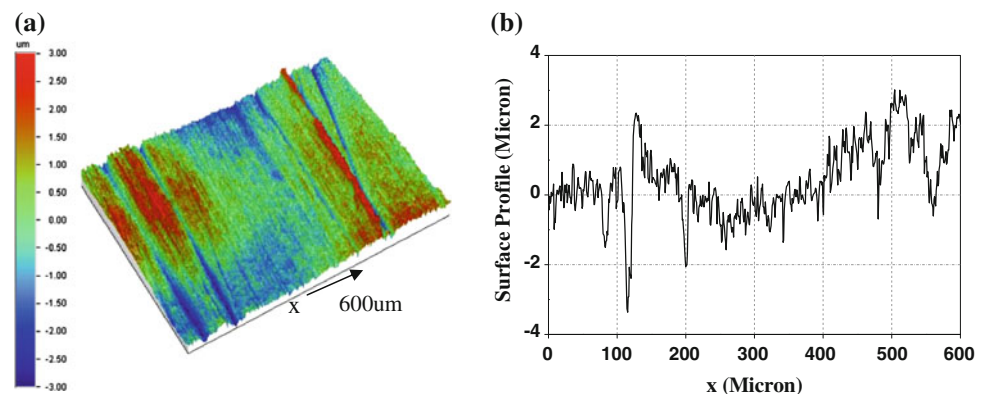


Fig. 4 Surface profile measurements on the polished microwave laminate. **a** 3D-image and **b** linear scan measurement

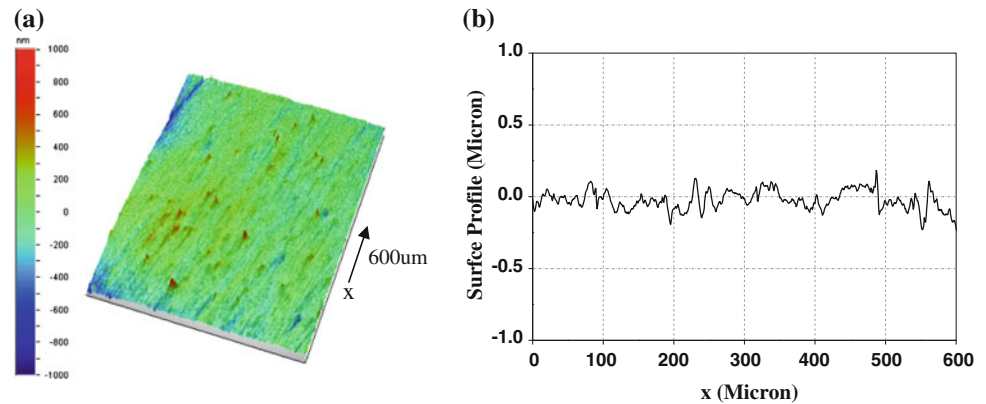
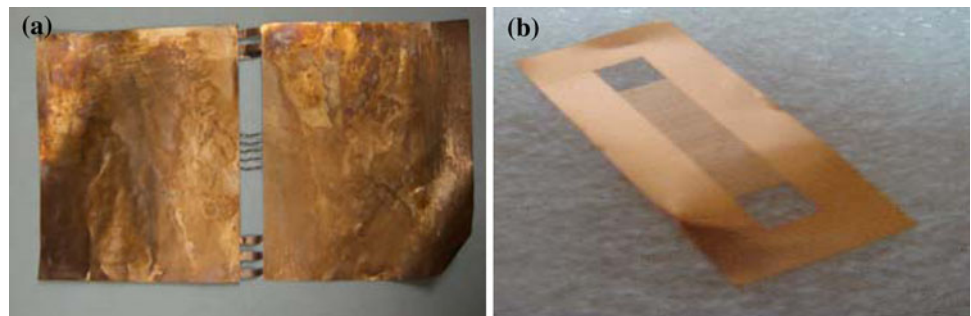


Fig. 5 **a** Bridges patterned on copper foil by wet chemical etching, **b** layer with bridges fabricated using photochemical milling



1 min and at 95°C temperature for 2 min. This process is repeated twice to get the SU-8 film of thickness 4 μm . Lithography is done using double side mask aligner with flood exposure of 220 mJ/cm^2 . After developing the sample is hard-baked for 30 min at 150°C.

3.3 Realization of beam structures

The bridge structure is patterned on a thin copper film/foil to lower the actuation voltage. Foil thickness of 15 μm is used so that pull-in voltage is about 100 V. Residual stress of this film causes wrinkles as shown in Fig. 5 during conventional wet lithography process. Therefore, an alternative approach using photo-chemical milling (PCM) is used to realize beam structures. In PCM, the etching is done in a multi-chambered machine that has driven-wheel conveyors to move the foils to be patterned, and arrays of spray nozzles above and below these foils. The etchant is typically an aqueous solution of acid, frequently ferric chloride that is heated and directed under the pressure on both sides of the foil. The etchant reacts with the unprotected metal, corroding it quickly. After neutralizing and rinsing, the remaining resist is removed and the sheet of parts is cleaned and dried. This approach can be used for materials of thicknesses ranging from 13 to 2,000 μm . The quality of foil profile is controlled by varying pressure, temperature, spray system, etchant concentration, or

distance between object and nozzle. Fig. 5 shows the beam structures realized on copper foil in which beam structures remain straight after patterning. This approach is also used to pattern the spacer layer which consists of a copper film with a rectangular window in the middle. Since both these layers are not formed by deposition and patterning, this phase shifter can be fabricated in a typical PCB manufacturing facility without the need for high cost thin film deposition equipment or processes.

3.4 Integration of the phase shifter

As discussed above, the two copper foils for spacer and bridge structures are aligned above the CPW on the microwave laminate. A plexiglass sheet of thickness 2 mm is used as the topmost layer to maintain the straightness of the membrane film as well as to provide protection to these. These layers are assembled together and held intact using four screws as shown in Fig. 6. As the top and bottom layers are rigid and are held in place by tightening the screws, the overall configuration can be assembled reliably and repeatedly with this approach. DC bias wires are attached by soldering at the uncovered ends of the device. The cross sectional view of the arrangement is shown in Fig. 7. It is evident that this is simple but reliable and repeatable. The phase shifter is characterized for electro-mechanical as well as RF performance in the next section.

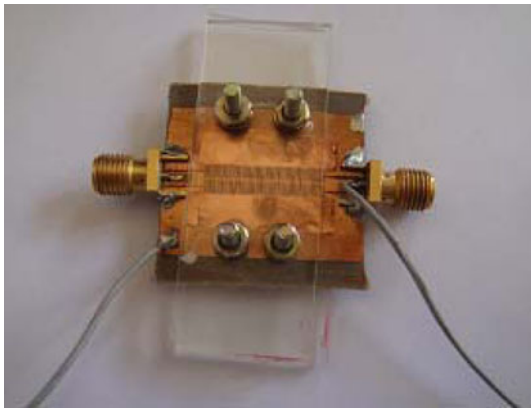


Fig. 6 Photograph of the complete phase shifter

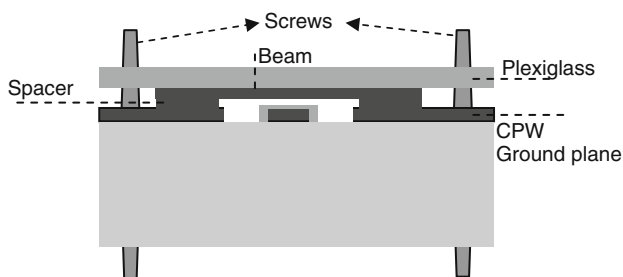


Fig. 7 Cross section of the integrated phase shifter

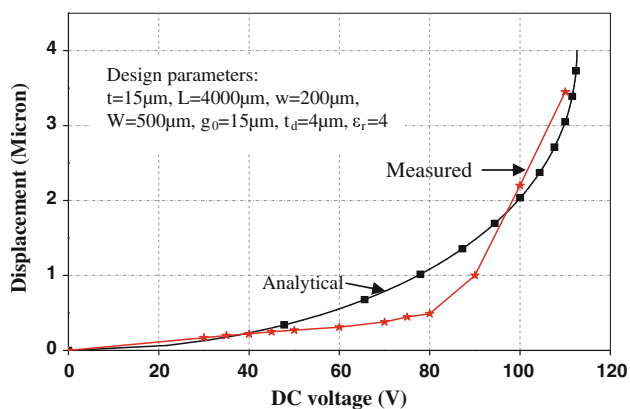


Fig. 8 Comparison in analytically modelled and measured deflection of the beam as the bias voltage is varied

4 Measured results

4.1 Electromechanical characterization

The integrated phase shifter is characterized to measure the beam deflection with DC bias voltage using a Laser Doppler Vibrometer (LDV), which is based on the principle of Doppler effect. The laser beam of the LDV is focused on the beam structures of the device and AC (peak to peak 10 V) plus variable DC bias is applied between the

signal and ground conductors of the CPW for electrostatic actuation of the beams. Although the final assembled device shown in Fig. 6 is completely covered with the plexi-glass to protect the bridges, samples prepared specifically for the mechanical characterizations are assembled with a cavity in the top plexiglass to enable the laser beam of the LDV to strike the beam structure. The displacement of this beam structure is noted for various the DC bias voltages. Fig. 8 shows a comparison of these measured results with analytically calculated values for deflection. Comparison in measured, simulated, and analytically modelled pull-in data is presented in Table 2 which shows that measured electromechanical behaviour of the beam structure is well matched with the simulated and analytical data.

4.2 RF characterization

The assembled phase shifter is characterized at the X-band frequency range using a vector network analyzer. Measured reflection loss of the device (Fig. 9) is better than -13 dB, and remain within this level for all applied voltages. The measured phase characteristics in Fig. 10 indicates that a phase shift of 48.5° with 85 V DC bias at 9.5 GHz. Gap below the bridge layer is calculated from the RF performance of the device is found to be $14.14\ \mu\text{m}$, which is close to the expected gap of $15\ \mu\text{m}$. It may be noted from Figs. 9 and 10 that due to minor variation in height, the impedance match changes and this causes the variation in phase shift not to be strictly linear with frequency.

Table 2 Comparison in pull-in data

Parameters	Values
Measured pull-in (V)	110
Coventorware simulation pull-in (V)	105.93
Analytically modelled pull-in (V)	112.56

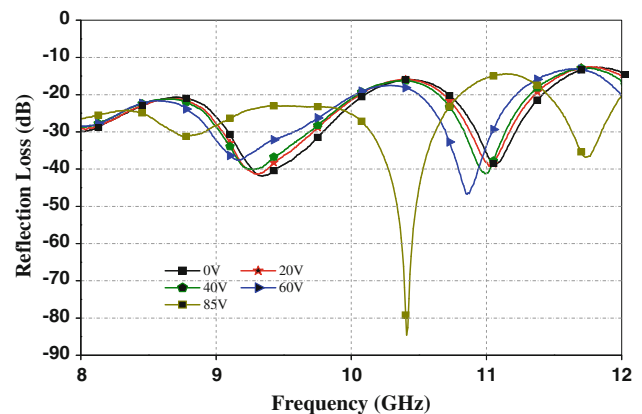


Fig. 9 Measured reflection loss of the MEPL

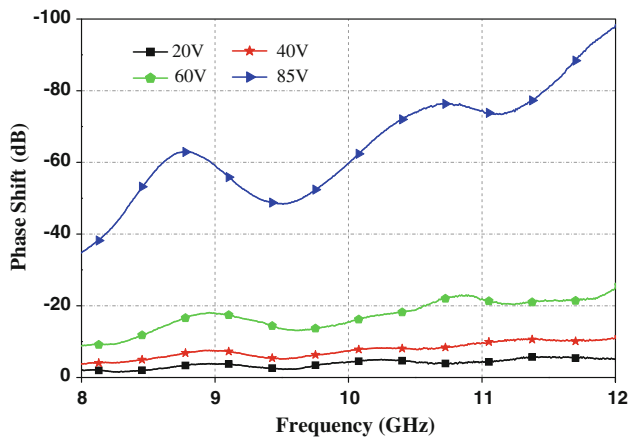


Fig. 10 Measured phase shift of the MEPL for different bias voltages

Table 3 Comparison in RF performance of two identically fabricated devices

At 10 GHz	Device 1	Device 2
Phase shift (°)	-60	-63
Reflection loss (dB)	-20	-20

Devices are fabricated and using this approach and tested for RF performance. Comparison in RF performance of two fabricated devices is presented in Table 3 which shows the reproducibility of the approach.

5 Summary

The mesoscale phase shifter demonstrated in this paper has several advantages compared to micromachined phase shifters. The proposed fabrication approach does not use metal deposition/patterning process, which eliminates the need of high cost cleanroom and sophisticated equipment for film deposition. Secondly, as the structural members in this phase shifter are not from deposited thin films, stiction

is not expected. Since this approach uses thicker metal films, the power handling capability is expected to be significantly higher than micromachined phase shifters. However, the present demonstration requires a high actuation voltage. Buck converters using charge pump circuits can be used to control this phase shifter in a digital control environment. This voltage requirement can possibly be reduced significantly by modifying the beam geometry using advanced lithographic approaches. As shown in Table 4, this approach has several differences compared to other similar approaches on laminates (Ramadoss et al. 2006).

Furthermore, this configuration of phase shifter on laminates offers new possibilities for monolithic integration of phase shifters with other components of phase arrays. Since conventional phased array antenna system components are fabricated on a microwave laminate, micromachined phase shifters realized on semiconductor substrates are required to be packaged separately before integrating with such phased array circuits. Packaging of the RF-MEMS/MEMS devices is still a major challenge and contributes to a substantial part of the total cost. Unlike micromachined phase shifters which are required to be packaged and then embedded in phased array applications, this device is packaged in situ. This reduces the cost and size of the array and improves its reliability and performance. Compared to similar monolithic phased array antenna reported on silicon substrate which is limited by wafer size, these arrays can be easily extended for large arrays on microwave laminate as these are available in large size.

To conclude, a simple low cost approach is proposed here for the fabrication of electrostatically actuated phase shifters. The basic design of this phase shifter inherits the advantages of low losses, wide bandwidth, low DC power consumption, and high linearity of MEMS phase shifters over those fabricated by semiconductor/MMIC technology. Furthermore, compared to micro-fabricated phase shifters which are not yet used widely because of issues related to

Table 4 Comparison in proposed and other similar approaches

	Reported (Ramadoss et al. 2006)	Proposed
Packaging	Packaging is required	Self packaged device as the top plexiglass lid acts as the package layer
Milling/Cutting	Milling machine and laser cutting machine are used in fabrication	No milling/cutting machines are used
Spacer	Polyflon adhesive layer is used as spacer which is dielectric. Spacer layer is milled to make holes for RF contact pads	Copper metal is used as spacer film
Assembling	Thermo-compression bonding technique is used	Repeatable results in the present approach without using bonding techniques
Metallization	Metal deposition is used for electrodes on kapton membrane	Metallization is not required as precast layers are used

their fabrication reliability, packaging, and integration, the proposed MEPL overcomes these issues, while retaining all the advantages of conventional MEMS phase shifters with the additional benefit of low cost. The entire fabrication process can be performed in a good PCB manufacturing facility without the need for high cost vacuum deposition equipment of processes in cleanrooms. Furthermore, these are integrable to form a monolithic phased array. The electrical and electromechanical performance parameters of the fabricated prototypes agree with simulations.

References

- Barker NS, Rebeiz GM (1998) Distributed MEMS true-time delay phase shifters and wide-band switches. *IEEE Trans Microw Theory Tech* 46(11):1881–1890
- Barker NS, Rebeiz GM (2000) Optimization of distributed MEMS transmission-line phase shifters—U-band and W-band designs. *IEEE Trans Microw Theory Tech* 48(11):1957–1966
- Borgioli A, Liu Y, Nagra AS, York RA (2000) Low-loss distributed MEMS phase shifter. *IEEE Microw Guid Wave Lett* 10(1):7–9
- Fangmin G, Zongsheng L, Guanglong W, Shouzheng Z, Ziqiang Z, Gengqin Y, Xiaohong G, Siqing C, Jiangfang X (2001) Millimeter wave phase shifters with periodically spaced MEMS bridges loaded. *IEEE* 2:769–772
- Ghodsian B, Jung C, Cetiner BA, Flaviis FD (2005) Development of RF-MEMS switch on PCB substrates with polyimide planarization. *IEEE Sens J* 5(5):950–955
- Guo F, Zhang Y, Lin J, Kong J, Zhu S, Lai S, Zhu Z (2006) MEMS phase shifters on low-resistivity silicon wafer. *Proceedings of the IEEE international conference on mechatronics and automation*, Luoyang, China, pp 497–501
- Hayden JS, Rebeiz GM (2000) 2-bit MEMS distributed X-band phase shifters. *IEEE Microw Guid Wave Lett* 10(12):540–542
- Hayden JS, Rebeiz GM (2002) A low-loss Ka-band distributed MEMS 2-bit phase shifter using metal-air-metal capacitors. *IEEE MTT-S Digest* 337–340
- <http://www.microchem.com/>
- Hayden JS, Rebeiz GM (2003) Very low-loss distributed X-band and Ka-band MEMS phase shifters using metal–air–metal capacitors. *IEEE Trans Microw Theory Tech* 51(1):309–314
- Lakshminarayanan B, Weller T (2002) Distributed MEMS phase shifters on Silicon using tapered impedance unit cells. *IEEE MTT-S Digest*
- Lakshminarayanan B, Weller TM (2006) Design and modeling of 4-bit slow-wave MEMS phase shifters. *IEEE Trans Microw Theory Tech* 54(1):120–127
- Lakshminarayanan B, Weller TM (2007) Optimization and implementation of impedance-matched true-time-delay phase shifters on quartz substrate. *IEEE Trans Microw Theory Tech* 55(2):335–342
- Liu Y, Borgioli A, Nagra AS, York RA (2000) K-band 3-bit low-loss distributed MEMS phase shifter. *IEEE Microw Guid Wave Lett* 10(10):415–417
- McFeetors G, Okoniewski M (2006) Distributed MEMS analog phase shifter with enhanced tuning. *IEEE Microw Wirel Compon Lett* 16(1):34–36
- Palei W, Liu AQ, Yu AB, Alphones A, Lee YH (2005) Optimization of design and fabrication for micromachined true time delay (TTD) phase shifters. *Sens Actuators A* 119:446–454
- Ramadoss R, Sundaram A, Feldner LM (2005) RF MEMS phase shifters based on PCB MEMS technology. *Electron Lett* 41(11):654–656
- Ramadoss R, Lee S, Lee YC, Bright VM, Gupta KC (2006) RF-MEMS capacitive switches fabricated using printed circuit processing techniques. *IEEE J Microelectromech Syst* 15(6):1595–1604
- Rebeiz GM (2003) RF MEMS theory, design, and technology. IEEE Press, New York
- Topalli K, Unlu M, Demir S, Aydin CO, Koc S, Akin T (2006) New approach for modelling distributed MEMS transmission lines. *IEE Proc-Microw Antennas Propag* 153(2):152–162
- Wang J, Ativanichayaphong T, Huang WD, Cai Y, Davis A, Chiao M, Chiao JC (2008) A distributed MEMS phase shifter on a low-resistivity silicon substrate. *Sens Actuators A* 144:207–212